MOLECULAR DYNAMICS SIMULATION STUDY OF EUCOMMIAULMOIDES GUM/AG NANOPARTICLE COMPOSITES

Fei-Zhou Li[1,2*], Zhen-Lin Lu[2],Yuntao Xi[4], Xin-shengWang[2], Ming-qiang Zhu[3]

[1]Baoji University of Arts and Sciences, Department of Mechanical, Baoji 721007, China.Xi'an
[2]University of Technology, School of Material Science and Engineering, Xi'an 710048, China.
[3]College of Forestry, Northwest A&F University, Yangling 712100, China.)
[4]School of Material Science and Engineering, Xi'an Shiyou University, Xi'an 710065, China

*Author to whom correspondence should be addressed: E-mail:lfz-1010@163.com

Received 25 April 2017; accepted 15 June 2017

ABSTRACT

A study of eucommia ulmoides gum (EUG)/Ag nanoparticle (NP) composites by molecular dynamics (MD) simulations to understand their structure, polarizability, thermodynamic properties, and mechanical properties is proposed. The effects of simulation temperature and Ag NPs size on these parameters were also studied. The results revealed that the composites exhibited an isotropic amorphous structure, and the distribution uniformity of the Ag NPs was enhanced by changing the simulation temperature. Several atoms of the Ag NPs were in an amorphous state, and a polarized layer was observed on the interface between the Ag NPs and the eucommia ulmoide matrix. The interface size increased as the temperature increased and nanoparticles size decreased. The isochoric heat capacity and thermal pressure coefficient of the EUG/Ag-NP composites exhibited significant size effects and improved thermal interferences, which indicated that the presence of the Ag NPs had a positive effect on the mechanical properties of the EUG.

Keywords: Molecular Dynamics Simulation, Ag Nanoparticle, Eucommia Ulmoides Gum

1. INTRODUCTION

Recently, significant advancements have been made in the study and synthesis of functional composites of Ag NPs and polymers [1, 2]. Owing to their unique electronic structure and ultra-large specific surface area (e.g., surface area of 160-640m^2/g for particle sizes of 15-20 nm in the distributed phase), Ag NPs have been used in chemical catalysis, surface enhanced ram an spectroscopy (SERS), sensing, bio-labelling, and anti-bacterial applications [3-5]. Polymers reported include eucommia ulmoides gum alcohol, polypyrrole, polystyrene, and polymethylmethacrylate (PMMA)[6,8]. Ag/polymer composites exhibit not only intrinsic characteristics of the Ag NPs and polymers, but also novel functions/properties that are not observed in either one by itself. Therefore, these composites are promising materials in various fields including photonics, electronics, biomedical industries, and information materials [9, 11]. Performance improvements of conventional micro-sized particle-filled polymer composites have been limited; improvements of certain properties always occur at the cost of degradation of other properties. For instance, the thermal and mechanical properties, and flame retardancy of conventional particle-filled polymer composites can be improved, but their electrical strengths become significantly reduced [12]. Once the size of filling particles is reduced below 100 nm, the polymer/nanoparticles composites exhibit significant improvements in their overall performance. For instance, establishment of nano-sized high-order structures in epoxy resin can retard phonon scattering and improve thermal conductance without sacrificing other properties, making it a multi-functional material. Meanwhile, dielectric withstanding voltage, spatial distribution of electric charges, and corrosion resistance of nano-composites are also improved [13].The effect of CdSe nanoparticles on the fluorescence spectra of conjugate polymer Ply(3-hexylthiophene-2,5-diyl)(P3HT) were investigated by experiment and simulated calculation, results showed the fluorescence intensity is significantly decreased in both solution and solid films by the incorporation of CdSe Nps and calculations were found to be in good agreement with the experimental data[14-16].Polymer/nanoparticles composites (also known as nano-dielectrics) are essentially a mixture of

nanoparticles and polymers, and their properties are determined by size, shape, distribution, filling area of nanoparticles, molecular weight of polymer molecules, and their interactions between the nanoparticles and polymer matrices[17].

EUG consists of natural polymers, often called Gutta-percha or Balata, that have the same chemical composition (C5H10) as natural rubber, but a different molecular chain configuration, which results in many different traits, it has good mechanical ,electrical insulation, thermal stability, acid and alkali, wear, super-hydrophobic, impact resistance and corrosion resistant properties, and has been widely applied in car tires, underwater cables, medical function rubber sheet and prosthetic , stealth materials of the submarine and ship[18,19]. In earlier time, EU gum was applied in manufacturing submarine cables, especially for use in the Atlantic Ocean. The huge demands for submarine cables accelerated the rapid development of EU gum industry. At one time, it reached an annual production of more than ten thousand tons [20]. Due to the rapid development of the synthetic plastics industry, EU gum gradually became phased out by inexpensive fossil products. However, with respect to the oil crisis, EU gum is again attracting increased attention. Developing EU gum as the second natural rubber resource has become the focus of interest of many researchers [21-23]. Usually, rubber has good mechanical properties, the purified form of natural rubber is the chemical polyisoprene, which can also be produced synthetically. Natural rubber can be used in many packaging products such as films and tapes[24]. In general, when elastomers are blended with other polymers, their physical and mechanical properties will be enhanced. Adding trans-1,4-polyisoprene (EU gum) in natural rubber is one of the mixtures of interest regarding that it is an ideal compatible blend with comparable glass transition temperature[25]. Rubber composites are mainly used for making ropes, hose, belt, and mats [26,27]. It is a biodegradable material which can disintegrate in soil by specific microorganisms. In the meantime, there is a simultaneous and growing interest in developing use of bio-based products that can reduce the dependence on fossil fuel and move to a sustainable materials basis[28,29]. This situation favours for unique bionanocomposites possessing wonderful properties, which have be never found in conventional composites, and biodegradable bio-based nanocomposites are supposed to be the next generation of materials for the future[30]. Last two decades, natural rubber was extensively applied as a matrix in the synthesis of bionanocomposites with polymers, such as chitin whiskers, cellulose whiskers extracted from Syngonanthus nitens (Capim Dourado), and rachis of palm tree. It is worthy of noting that the as-prepared bionanocomposites usually exhibit higher mechanical properties. Bras et al.[31]had synthesized bagasse cellulose whiskers reinforced natural rubber nanocomposites films, using cellulose whiskers (84-102 nm in length and 4-12 nm in width) as reinforcing elements and natural rubber as a matrix. Moreover, rubber is endowed with extensive application at acoustics field by its superior acoustic characteristics. The acoustics impedances of most of rubbers can match that of water, and cannot match that of air. So rubber could be used as sound absorption materials in the water, and used as sound insulation materials and shock absorption materials in the air [19].

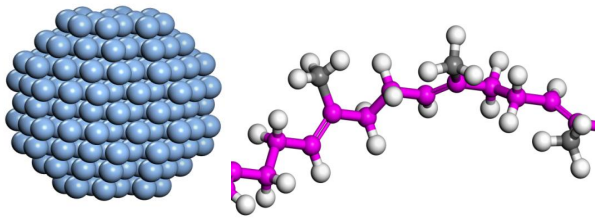
Performance improvements can only be achieved with certain distributions of nanoparticles in the polymer matrix. Molecular dynamics (MD) simulation investigates structures and time-variant motion of molecules/atoms based on motion equations of interacting molecules/atoms calculated by computer and deduce macroscopic characteristics of these materials. MD simulations can precisely replicate nanoscale systems consisting of various molecules and/or atoms, thus obtaining results that are barely achievable by experimentation[18]. Owing to their unique physical properties, polymer/Ag-NP nanocomposites have shown great potential in electric insulation, anti-bacteria, self-cleaning, thermal stability, and blending reinforcement[32]. Nevertheless, it is extremely challenging to understand the molecular mechanism of the polymer/Ag-NP compositing effect. As a key method for material modification and design, MD simulation has been applied in studies of polymer nano-dielectrics. In this study, a MD simulation study of EUG/Ag-NP composites using Materials Studio was proposed. A systematic analysis of these composites was achieved, and a comparison between these composites and eucommia ulmoides gum was conducted, Which provides a useful way to understand the function properties polymer/nano-composites and exploits the potential of the nanometre effect applied to polymer/nanocomposites.

2. MOLECULAR DYNAMICS SIMULATION METHODS

Nowadays, Materials Studio (condensed phase optimized molecular potentials for atomistic simulation studies) is one of the most recent and powerful

force fields developed for the study of condensed phase systems. MD simulations were performed to study the atomistic models of EUG /Ag blends using Material Studio. Firstly, minimized energy-targeted structure optimization of EUG molecules and Ag NPs (or clusters)comprising the nano-composites was achieved using the Discover module of Materials Studio. Then, amorphous unit cells were established based on optimized molecule/atom groups using the Amorphous Cell module to facilitate their simulation [33,18]. The amorphous unit cells were modified and system temperatures were set at 298 K, 350 K, 450 K, and 600 K. Energy optimization, structure optimization and MD simulation of established amorphous nano-composites were achieved using the Forcite module. Herein, van der Waals (VDW) forces and coulomb interactions in these composites were calculated using the atom radical summation method based on semi-empirical quantum mechanics PCFF force field that is suitable for polymers and various transition metals. The cutoff distance and buffering width were 12.50 Å and 1.50 Å, respectively. Structure optimization was achieved using the conjugate gradient method with an energy converging level of 1×10-5kcal/mol and maximum iteration step of 2×104. In the MD simulations, isothermal-isobaric (NPT) ensemble (fixed particle amount, pressure, and temperature) was employed, and the temperature was fixed in the range of 298-600 K using the Nosé–Hoover thermostat method. The step was set as 1×104, the time step was set as 1.0 fs, the simulation duration was set as 100.0 ps, and the integration tolerance energy shift was set as 5000.0 kcal/mol[32,34].

Three different nano-composites were established using spherical single crystal Ag-NPs with diameters of 10Å, 16Å, 20 Å and 30Å (with 38, 135, 236 and 856 atoms, respectively, and point symmetry group) and randomly distributed the EUG molecules[34]. Fig. 1 shows the optimized the EUG molecular structure related to Ag NPs with a diameter of 20 Å. Specific steps of the simulating method see in Fig.2. Based on the track data obtained by the MD simulation results, structure (cell parameter, density, and radial distribution of atoms), energy (potential energy, electrostatic energy, and VDW energy), dynamics (correlation functions), and mechanical properties of the composites were calculated using the Analysis tool in the Discover module and the Forcite module. Additionally, molecular mechanics and molecular dynamics of amorphous EUG were also obtained in order to investigate changes of the EUG after compositing with Ag NPs (in other words, the effects of Ag NPs on the EUG).



a. Ag nanoparticles (20 Å) b. The long eucommia ulmoides gum chains

Fig. 1: (a) Optimized Ag NPs with diameters of 20 Å and (b)Long chainEUG.

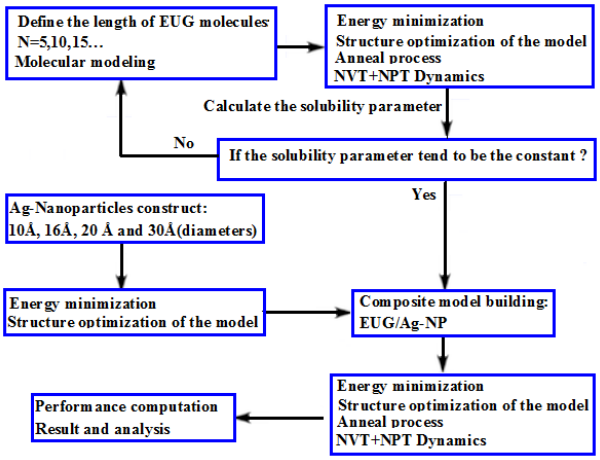


Fig. 2: Flow chart illustrating the molecular model developed to optimize EUG/Ag-NP structures

3. RESULTS AND DISCUSSION

3.1 MD simulation process

The energy and temperature of various systems in MD simulations were altered to verify the formation of a confirmed statistical ensemble Fig. 3 shows trends of overall energies and transient temperatures of EUG/Ag(20 nm)-NP and EUG at different simulation temperatures. As can be seen, variations were observed in 10.0-20.0 ps and the temperature and the frame trace energy fluctuated within ±10K and 0.1%~0.5%, respectively, indicating equilibrium states of these systems [14]. Hence, it can be concluded that thermodynamic equilibrium structures of these systems under designated conditions were achieved rapidly, and the internal energy and transient temperature of equilibrium systems fluctuated slightly around certain averages (thermodynamic equilibrium temperature). Owing to the isothermal control by NPT ensemble (fixed particle amount, pressure, and temperature), slight variations of internal potential energy and kinetic energy were observed. The transient temperature (particle velocity/kinetic energy) of the system had to be adjusted continuously to ensure the statistical averages and standard deviations met the requirements of thermo-

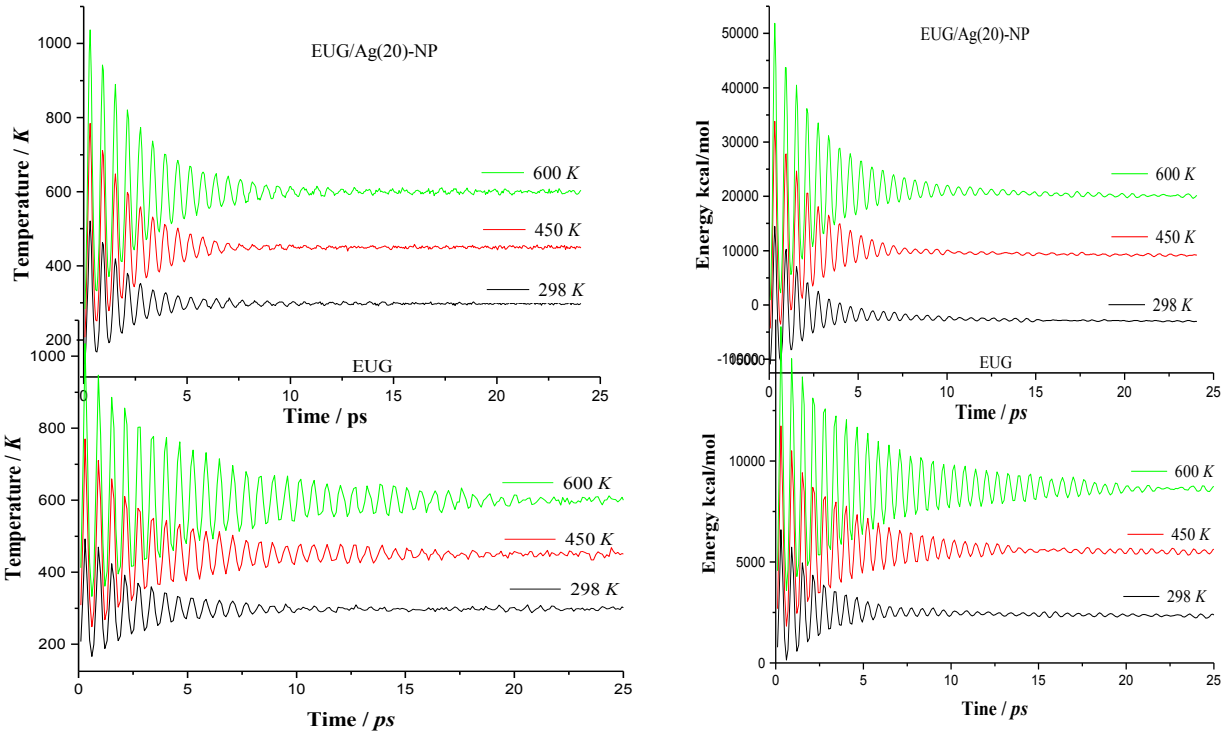


Fig. 3: Energy and temperature in MD simulation of EUG/Ag (20Å)-NP and EUG vs. time.

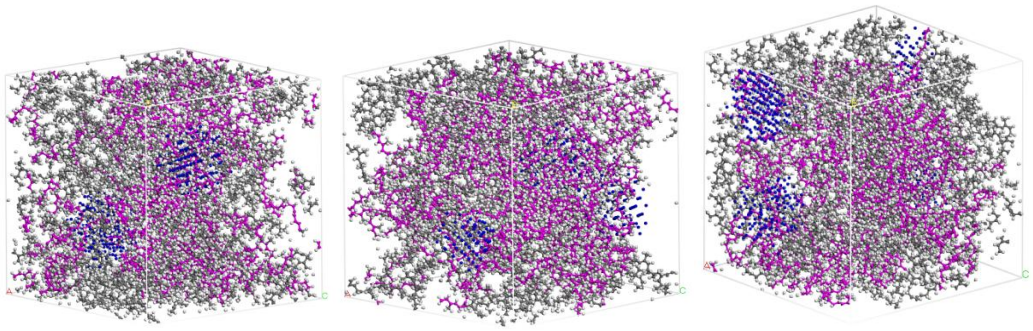
dynamic temperature control. Also, it was easier for nano-sized EUG/Ag-NP composites to reach equilibrium; the duration to reach equilibrium increased as the temperature increased. These results indicated that the MD simulations satisfied the predetermined statistical ensemble conditions, and the thermodynamic fluctuations in the simulations were statistically significant.

3.2 Structure

Fig. 4 shows equilibrium structures of EUG/Ag-NP composites at 298 K and 600 K obtained by MD simulations. Table 1 summarizes the composition of amorphous unit cells of EUG/Ag-NP composites

Table 1: Composition of EUG/Ag-NP composites.

Sample	Diameter of Ag NPs (Å)	Number of EUG chains (n = 50)	Number of Ag NPs	Atomic number of composites (except H)	The Ag NPs content
a	10	11	4	2750/152	30%
b	16	20	2	5000 /272	30%
c	20	36	2	9000/464	30%
d	30	127	2	31750/1336	30%



(a) 298 K (b) 350 K (c) 450 K

Fig. 4: Equilibrium structures by MD simulations (Ag atoms = blue, C atoms = violet and grey, H atoms = white)

with different Ag NPs size. The content of Ag-NPs in all the samples was 30%. As can be seen, aggregations of Ag NPs were observed at 298 K, which indicated poor distribution uniformity of Ag NPs in amorphous unit cells of EUG/Ag-NP composites. As the simulation temperature increased, the distribution uniformity of the Ag NPs in the EUG matrix increased, demonstrating that the distribution uniformity of the nanoparticles were significantly enhanced by increasing the temperature.

Table 2 lists a summary of the energy of the EUG/Ag-NP composites and EUG systems at 350 K in the MD simulations. As can be seen, the VDW energy and total potential energy of the composites were significantly lower than those of the EUG systems. Meanwhile, the total potential energy increased as the NP size decreased, which indicated that the Ag NPs and EUG matrix were held together by strong VDW forces (dispersion forces). As a result, the total energy was drastically reduced and the structural stability was significantly enhanced. In other words, material modification was achieved.

Fig. 5 shows the atomic surface density distribution functions of the EUG/Ag(20)-NP composites and EUG system (298 K) in different directions. The atomic surface density distribution curves of (100), (010), (001) crystal faces of the amorphous unit cell fluctuated around the same value, which indicated that the system was an amorphous structure with random atomic surface density distribution. Additionally, the atomic surface density of the EUG/Ag(20Å)-NP composites varied significantly with lattice distance, while variations of that of the EUG systems were negligible.This was attributed to the relatively high atomic surface density of the Ag NPs. On the other hand, this is related to the nanometre effect of Ag particle, which the high surface passivation effect and the quantum effect with a strong character of confinement of electrons and holes at nanometre scale in all space directions results in the concentration profile of Ag NPs are fluctuated obviously. Meanwhile, the density of the Ag single crystals was significantly higher than that of the EUG, and the bonding of the Ag NPs and EUG molecules were strong (see Figure 5b), resulting in a significantly increased density of the composites. Owing to the constant contents of Ag NPs in different samples, densities of these samples were consistent with each other, as shown in Table 2.

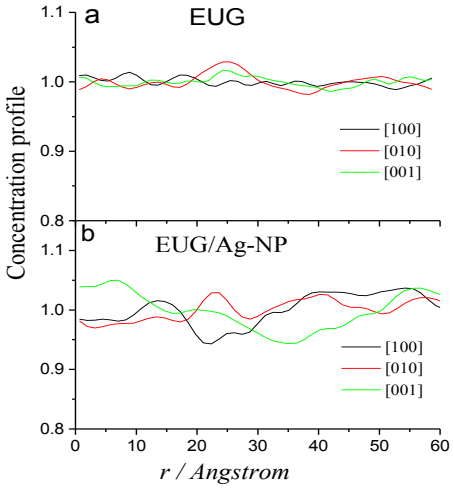


Fig. 5: Atomic surface density distribution function of EUG/Ag(20)-NP composites and EUG system (298 K).

Fig.6a, b, and c show the radial distribution functions of C-C bonds and Ag-Ag bonds in the equilibrium structure of the EUG/Ag(20)-NP composites, C-C bonds in the equilibrium structure of the EUG system, and Ag-Ag bonds in the equilibrium structure of Ag single crystals, respectively, all at 298 K. Four and three characteristic peaks were observed in the radial distribution functions of C-C bonds in

Table 2: Energy compositions and densities of EUG/Ag-NP composites and EUG system at 298 K.

Energy (kcal/mol)	EUG/Ag(10)-NP	EUG/Ag(16)-NP	EUG/Ag(20)-NP	EUG/Ag(30)-NP	EUG
VDW energy	-4642.259	-9143.058	-16607.269	-55444.7	-1016.87
Electrostatic energy	-2512.517	-4572.783	-8226.666	-6823.566	-1135.949
Kinetic energy	-1956.52	-3288.7	-5602.93	-5608.57	-750.381
Potential energy	-7154.765	-13715.8	-24833.935	-62268.23	-2152.819
Total energy	-9111.285	-17004.5	-30436.865	-67876.8	-2903.2

the EUG/Ag(20)-NP composites and EUG systems, respectively, in areas within 4 Å, while no peaks were observed beyond 4 Å in any of the samples. Additionally, the characteristic peaks of C-C bonds in the EUG systems revealed that these systems were amorphous structures with short-chain ordered and long-chain disordered characteristics, as shown in Fig. 6 a. Three peaks were observed in the radial distribution functions of C-C bonds in the EUG/Ag-NP composites, and their positions were consistent with those of the EUG systems. Their intensities were significantly higher and one additional peak was observed, which was attributed to changes of C-C bonds in the EUG molecules that were close to the Ag NPs. As shown in Fig. 6c, several peaks were observed in the atomic radial distribution functions of 20Åsingle crystal Ag NPs. These peaks corresponded to periodically arranged Ag atoms, indicating periodicity of atom arrangement in the Ag NPs. Intensities of these peaks were significantly lower than that of the peaks shown in Fig. 6b, and those at the far ends exhibited negligible intensities. These results indicated that the periodic arrangement of the Ag atoms in the nano-composites was not eliminated by the EUG matrix, although the periodicity was affected in certain ways and the surface Ag atoms were in amorphous states. Also, the EUG was still in an amorphous state. Additionally, the interface area (areas without peaks in radial distribution functions of Ag-Ag bonds) in the Ag NPs increased as the NPs size decreased and temperature increased.

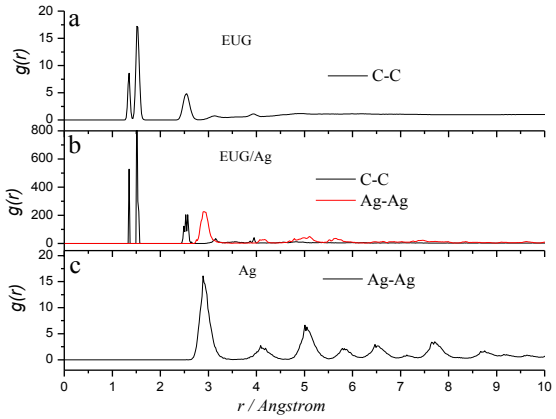


Fig.6: Radial distribution functions of the equilibrium structure of(a) EUG/Ag(20)-NP composites, (b)EUG system, (c) Ag NPs (simulation temperature = 298 K).

3.3 Thermodynamic properties

Thermodynamic parameters (e.g., heat capacity, insulating coefficient, and thermal compressibility) of the EUG/Ag-NP composites and EUG were obtained based on statistical analysis of MD simulations. Fig. 7 shows the isochoric molar heat capacities of the EUG/Ag-NP composites and EUG at different simulation temperatures. As can be seen, the heat capacity of the EUG/Ag-NP composites was higher than that of the EUG samples. Furthermore, the heat capacities of all samples increased with simulation temperature and NPs size, while the effects of NPs size were more significant. As the Ag NPs diameter decreased, the surface area and surface energy of these NPs increased drastically. This could be attributed to the increasing percentage of surface Ag atoms as a result of the decreasing NP diameter. Surface atoms are different from internal ones in terms of crystal field environment and combination energy. Owing to dangling bonds caused by the absence of adjacent atoms, surface atoms exhibit unsaturated characteristics and can readily combine with nearby EUG molecules, resulting in variations of thermal vibration resistance commonly observed in single crystal Ag atoms. As a result, effects of temperature and NP size on heat capacity are more significant for nano-composites.

Molecular dynamics simulation of analysis of quantum fluctuations can calculate thermodynamic quantities, such as heat capacity, adiabatic and heat pressure coefficients. Isometric heat capacity, C_V is calculated by total energy, E_T or potential energy, U at NVT ensemble[34].

$$C_V = \frac{\langle E^2 \rangle - \langle E \rangle^2}{k_B \langle T \rangle^2} = \left[\frac{\langle U^2 \rangle - \langle U \rangle^2}{k_B \langle T \rangle^2} + \frac{D_f k_B}{2} \right] \quad (1)$$

k_B is Boltzman constant, D_f is the system degrees of freedom, T is temperature. Fig. 8 shows isochoric heat pressure coefficients of the EUG/Ag-NP composites and EUG at different simulation temperatures and NPs size. As observed, the absolute values of heat pressure coefficients of the EUG/Ag-NP composites were significantly higher than those of the EUG samples. The heat pressure coefficients of the EUG/Ag-NP composites did not vary significantly with simulation temperature, indicating negligible effects of simulation temperature on the heat pressure coefficients of the EUG/Ag-NP composites and good thermal stability of the proposed composites. Therefore, it was reasonable to conclude that composition of the Ag NPs had a positive effect on the thermal resistances of the composites. Additionally, the size effect of thermal pressure coefficient was significant as it decreased drastically as the NPs size increased.

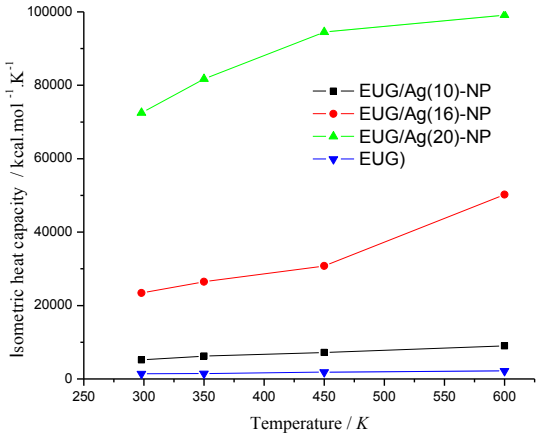


Fig. 7:. Relationship between isometric heat capacity and temperature.

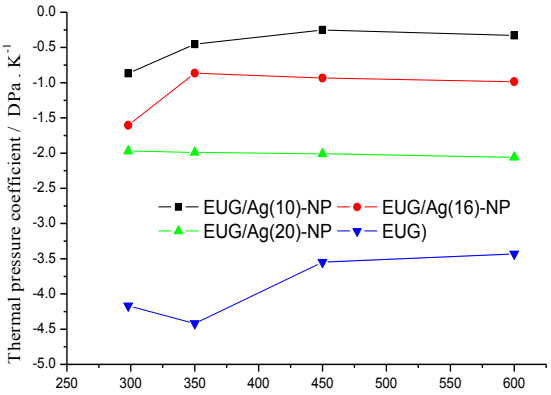


Fig. 8: Relationship between thermal pressure coefficient and temperature.

3.4 Polarizability

The polarizabilities of the EUG/Ag-NP composites and EUG samples in the MD simulations were calculated using the Protocols tool in the Amorphous Cell module. The diagonal elements of polarizability tensors obtained at an external electric field of 107 V/m were consistent with each other while other elements were negligible. In other words, these samples were highly isotropic. Fig. 9 shows the polarizabilities of different samples at different simulation temperatures. As observed, the polarizabilities of the EUG/Ag-NP composites were significantly lower than those of the EUG samples and decreased as simulation temperature and NPs size increased. It was, therefore, deduced that the interface layer between the Ag NPs and EUG molecules (spatial scale decreased as simulation temperature increased) had a positive effect on the dielectric performances of the composites.

3.5 Mechanical properties

According to general Hooke's law, 36 matrix ele-

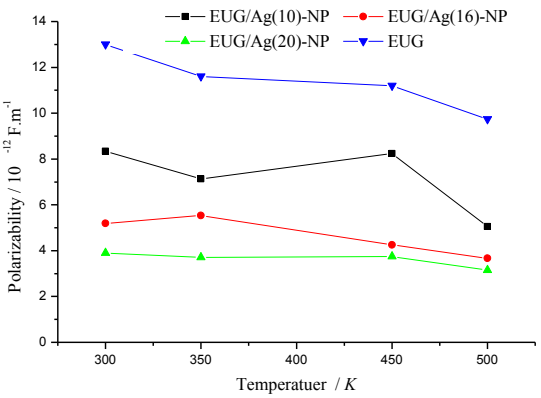


Fig. 9: Polarizability of EUG/Ag(20)-NP composites and EUG vs. simulation temperature.

ments in elastic coefficient Cij (6×6) can describe the general correlation of stresses and strains under deformations. Essentially, all mechanical properties can be deduced from the elastic coefficient matrix. Owing to the elastic strain energy, only $C_{ij} = C_{ji}$(or in other words, 21 individual elastic coefficients)is valid, even for extreme anisotropic materials. As shown in Table 3, values of elements other than the diagonal elements (C_{ii}) and C_{12}, C_{13}, C_{23}were negligible, indicating that both EUG samples and EUG/Ag-NP composites are orthotropic anisotropic elastomers [33].The C_{11} and $C_{22}$of EUG were relatively large (suggesting that large stresses are required to generate certain strains), while other coefficients were relatively low, indicating anisotropic properties of the EUG crystals. Compared with EUG samples, the EUG/Ag-NP composites exhibited decreased C_{11}, C_{12}, C_{13} and increased C_{33}, C_{44}, C_{66}, demonstrating that composition of Ag NPs leads to increasing isotropy. Also, the Poisson's ratio of EUG/Ag-NP composites was lower than that of EUG samples. Therefore, it was concluded that the composition of the Ag NPs had a positive effect on the mechanical performance of EUG.

4. CONCLUSIONS

A study of EUG/Ag-NP composites by molecular dynamics (MD) simulations was conducted to understand their structure, polarizability, thermodynamic properties, and mechanical properties, and the effects of NPs size and simulation temperature on these parameters was investigated. Using the NPT ensemble, trends of energies and temperatures of different systems at different temperatures against time were simulated. The results revealed that thermodynamic equilibrium structures (convergence) of all systems were achieved rapidly, and the composites reached equilibrium faster than the EUG and Ag NPs. Distribution uniformity of the

Table 3: Mechanical properties of EUG and EUG/Ag-NPs composites (GPa).

Elastic modulus	EUG/Ag-NP (10 Å, 298 °C)	EUG/Ag-NP (16 Å,298 °C)	EUG/Ag-NP(20 Å, 298 °C)	EUG (298 °C)	EUG/Ag-NP (10 Å, 350 °C)	EUG/Ag-NP (10 Å, 450 °C)
C_{11}	2.8462	0.0416	0.717	9.5	1.5538	1.5538
C_{22}	3.5272	3.7006	1.925	3.2082	0.8184	-0.5974
C_{33}	1.9591	3.222	0.8339	0.079	3.5613	1.9601
C_{44}	0.4137	0.977	0.4172	-0.888	1.1786	0.0694
C_{55}	1.2287	0.7209	-0.3056	0.319	2.5437	2.2055
C_{66}	1.2585	0.6899	0.4815	0.4217	0.7289	-0.4424
C_{12}	0.8623	1.094	-0.054	4.44	1.7652	1.2937
C_{13}	0.806	1.0472	0.1679	4.86	1.6829	1.9949
C_{23}	1.2879	1.7427	0.354	0.7341	1.3977	0.9948
C_{15}	-0.376	-0.1003	0.0814	-0.6007	0.3829	0.0316
C_{25}	-0.1062	0.2476	-0.0105	0.0689	-0.0205	-0.0156
C_{35}	-0.2909	0.1238	0.0264	-0.19	-0.1066	0.0081
C_{46}	-0.0139	0.0107	0.1509	0.0546	0.0175	-0.0898
Poisson's Ratio	0.1722	0.1960	0.2468	0.4472	0.3284	0.446
Elastic Modulus	71.3	0.576	0.068	0.699	0.872	0.1372

Ag NPs in the composites were significantly enhanced by temperature increases. The polarizability of the EUG/Ag-NP composites was lower than that of the EUG, and decreased as the temperature and content of the Ag NPs increased. The significant size and temperature effects of the interlayer areas played a key role in determining properties of the nano-composites. The isochoric heat capacity of the EUG/Ag-NP composites was higher than that of the EUG, increased with temperature, and was significantly affected by NPs size. However, the thermal pressure coefficient of the EUG/Ag-NP composites was negative and the absolute value was lower than that of the EUG. Also, the thermal pressure coefficient of the composites decreased significantly as the NP size increased; however, it was not affected by temperature. The Poisson's ratio of the EUG/Ag-NP composites was significantly lower than that of the EUG, and both increased with Ag NPs size and temperature. The elastic modulus of the EUG/Ag-NP composites decreased as the Ag NPs size and temperature increased. In summary, the composition of Ag NPs in the EUG systems result in the improvement of a variety of properties.

ACKNOWLEDGEMENTS

The authors gratefully acknowledge the State Forest Administration of China (Grant, No.948-2015459), the Science and Technology Program of China's Shaanxi Province (Industrial Key Technologies R&D Program, Grant, No. 2015GY146), the Education Department of China's Shaanxi Provincial Government (Science and Technology Development Plan, Grant, No. 15JK1209) for the research grant, and Northwest A&F University for supporting most of the materials and instruments used in this work.

References:

1. Lu L., Kobayashi A., Tawa K., et al. Chem .Mater., 2006 , 18 (20):4894-4901
2. Nikonorova N. A., Barmatov E. B., Pebalk D. A., et al. J. Phys. Chem. C, 2007 , 111(24):8451-8458
3. Haynes C. L., Mcfarland A. D., van Duyne R. P. Anal. Chem., 2005, 77(17): 338A-346A.
4. Aslan K., Lakowicz J. R., Geddes C. D. J. Phys. Chem. B, 2005, 109(13):6247-6251.
5. Panacek A., Kvitek L., Prucek R., et al. J. Phys. Chem. B, 2006, 110(33):16248-16253.
6. Mbhele Z. H., Salemane M. G., van Sittert C. G., et al. Chem. Mater., 2003 , 15(26): 5019-5024.
7. Pinter E., Patakfalvi R., Fulei T., et al. J. Phys. Chem. B, 2005, 109(37): 17474-17478.
8. Pinter E., Fekete Z., Berkesi O., et al. J. Phys. Chem. C, 2007, 111: 11872-11878.
9. Reda T., Collings F., Barton C., et al. J. Phys. Chem. B, 2003, 107(50): 13774-13781.

10. Panigrahi S., Praharaj S., Basu S., et al. J. Phys. Chem. B, 2006, 110(27): 13436-13444.
11. Barmatov E., Pebalk D., Barmatova M..Langmuir, 2004, 20(25): 10868-10871.
12. Ueki M., Zanin M..Trans. IEEE DEI, 1999, 6 876.
13. Li L., Wang X., Sun W., Lei Q..Acta Phys., 2013, 62(10) 106201-9.
14. N. Mastour, H. Bouchriha, Physics Letters A,2016,380 (2): 3866–3869.
15. N. Mastour, R. Ridene, H. Bouchriha. International Journal of hydrogen Energy ,2016,16(11):1-5.
16. N.Mastour,H.Mejatty,H.Bouchriha. Superlatticeand Microstructure,2015,82:461-471
17. A.Ben Ahmed,H.Saidi,S.Ridene,etc. IEEE Journal of Quantum Electronics,51(5):2500108e15
18. Fei-Zhou Li , Zhen-Lin Lu, Dong-Ping Tian. Polymers &polymer composits,2017,25(1):87-92.
19. Zhang, Ji. ZhaoHong Xue. polymer bulletin,2011,67(3):511-525.
20. Yan, R. F., in J.C. Salamone (Ed.). Polymeric materials encyclopedia, vol. 3, CRC Press, Boca Raton, 1996, p. 2291.
21. Tangpakdee, J., Tanaka, Y., Shiba, K.I. Phytochemistry,1997,45(1):75-80.
22. Qian, R. Y., Wu, Z.C., Xue, Z. H., Yan, R. F. Macromol. Rapid Commun. 1995,16(1):19.
23. Shinya, T., Takeshi, B., Yoshihisa, N., Biocsi. J.,Bioeng, 2008,105(4):355-359.
24. Bhowmick, A. K., Kuo, C.C., Manzur, A., et al. J Macromol Sci-Phys 1986; B25(3):283.
25. Julien Bras, Mohammad L. Hassan, Cecile Bruzesse., et al. Industrial Crops and Products. 2010,32:627-633.
26. Haghighat, M., Zadhoush, A., Khorasani, S. N. Journal of Applied Polymer Science,2005, 96(6):2203-2211.
27. Habibi, Y., Lucia, L.A., Rojas, O.J. Chemical Reviews, 2010,110(6):3479-3500.
28. Pandey, J. K., Kumar, A. P., Misra, M., Mohanty, A.K., Drzal, L.T., Singh, R.P., Journal of Nanoscience and Nanotechnology, 2005, 5(4): 497-526.
29. Dufresne, Alain. Canadian Journal of Chemistry,2008, 86(6): 484-494.
30. Siqueira, G., Abdillahi, H., Brass, J., Dufresne, A. Cellulose, 2010,17(2), 289-298.
31. Bras, Julien., Hassan, Mohammad. L., Bruzesse, Cecile., Hassan, Enas. A., EI-Wakil, Nahla. A., Dufresne, Alain. Industrial Crops and Products. 2010, 32, 627-633.
32. Li Fei-Zhou, Lu Zheng-Lin, Yang Zhi-Huai, Qi Kai. POLIMERY,2015, 60(7):45-48
33. Liao L., Fu Y., Liang X.Journal of Molecular Science, 2012, 28(6): 506-511.
34. Lin Li, Xuan Wang, Wei-Feng Sun, Qing-Quan Lei. Acta Phys. Sin,2013,62(10):106201e9